

# Damage Analysis of Resin-Based Fiber Composites Under Hygrothermal Coupling and Load-Hygrothermal Coupling Environment

SHI Jianjun\*, WANG Wenzhe, WEI Wangcheng, LIU Yifan

School of Civil Engineering and Architecture, Southwest University of Science and Technology,  
Mianyang 621010, P. R. China

(Received 10 March 2023; revised 6 September 2023; accepted 12 September 2023)

**Abstract:** The paper studies the damage of epoxy resin-based carbon fiber reinforced polymer (EP-CFRP) under the coupling effects of high and low temperature, humidity, tensile load. Two high and low temperature cycle intervals ( $[-40-40\text{ }^{\circ}\text{C}]/[-40-25\text{ }^{\circ}\text{C}]$ ), two humidity conditions (soaking in water/anhydrous), and three load levels (unstressed state/30% and 60% of the ultimate load) and their coupling effects are considered. The results indicate that all these three factors have a significant impact on the durability of EP-CFRP. The coupling effects of these factors have strong influence on the tensile strength, while affect little on the tensile modulus. The micro-cracks, which generated at the interface of the resin matrix and the fiber, have been proved to be the main reason for the strength reduction at later stage. The coupling effect of humidity and tensile load promote the expansion of cracks and exacerbates the damage to EP-CFRP. Based on the cumulative damage theory, the residual strength damage model of EP-CFRP under the three-factor coupling action of “high and low temperature cycle-humidity-load” is calibrated by nonlinear fitting method.

**Key words:** carbon fiber reinforced polymer(CFRP); high and low temperature cycle; humidity; tensile properties; residual strength model

**CLC number:** TN925      **Document code:** A      **Article ID:** 1005-1120(2023)S1-0138-13

## 0 Introduction

Carbon fiber reinforced polymer (CFRP) is extensively utilized in the aerospace, wind energy, and renewable energy sectors, owing to its impressive combination of high specific strength, exceptional specific modulus, lightweight properties, and formidable strength<sup>[1]</sup>.

Ambient temperature has a noticeable impact on the characteristics of resin-based composites. In a study conducted by Gao et al.<sup>[2]</sup>, the effects of thermal cycling within the range of  $[25-120\text{ }^{\circ}\text{C}]$  on the tensile strength of T700/3234 composites were investigated. The results indicated that, initially, the tensile strength of the composites decreased due to

the differences in coefficient of thermal expansion (CTE) between carbon fiber and the epoxy resin matrix, as well as the post-curing effect. However, after 50 cycles, the tensile strength started to increase and eventually stabilized after 100 cycles. Yu et al.<sup>[3]</sup> conducted measurements of the mechanical properties of CFRP after thermal cycling within the range of  $[-140-140\text{ }^{\circ}\text{C}]$ . The results revealed that as the number of thermal cycles reached 95, the transverse tensile strength experienced a reduction of 9%, after which it tended to stabilize. Meng et al.<sup>[4]</sup> discovered that internal defects in unidirectional CFRP composites became more pronounced after thermal cycling within the range of  $[-196-23\text{ }^{\circ}\text{C}]$ . After 150 cycles, the tensile strength decreased by

\*Corresponding author, E-mail address: jianjun\_shi@swust.edu.cn.

**How to cite this article:** SHI Jianjun, WANG Wenzhe, WEI Wangcheng, et al. Damage analysis of resin-based fiber composites under hygrothermal coupling and load-hygrothermal coupling environment[J]. Transactions of Nanjing University of Aeronautics and Astronautics, 2023, 40(S1): 138-150.

<http://dx.doi.org/10.16356/j.1005-1120.2023.S1.013>

approximately 2.4%. Lord et al.<sup>[5]</sup> observed that, after thermal cycling within the range of [−51—140 °C], the most severe matrix cracking took place during the initial 10 cycles, and then gradually diminished. Notably, around the 100th cycle, clear delamination of the material became evident. These studies collectively highlight the impact of high and low temperature cycling on the tensile properties of carbon fiber-reinforced composites. The used specific type of material, the temperature range encompassed by the cycling, and the duration of the cyclic process all emerge as critical factors influencing the degradation of performance in resin matrix composites.

Humidity is another significant factor affecting the properties of resin-based composites. In an investigation conducted by Li et al.<sup>[6]</sup>, mechanical behavior of CFRP under varying humidity conditions was studied using molecular dynamics simulations. It was observed that humidity resulted in a weakened interfacial adhesive performance. Ref.[7] reached a similar conclusion, proposing that moisture infiltrates the interface through an adsorption process, thereby accelerating the degradation of adhesive properties. Chen et al.<sup>[8]</sup> also noted bond strength degradation in the CFRP-concrete interface when exposed to a hot-wet environment. Plessix et al.<sup>[9]</sup> exposed EP-CFRP to an environment with relative humidity of 56%, 70%, and 84%. The experiment demonstrated that the higher the relative humidity, the faster the moisture absorption rate and the higher the moisture absorption rate. Yalagach et al.<sup>[10]</sup> further discovered that the diffusion coefficient and saturation mass of the composite increased with rising temperature and humidity. Collectively, the findings of these scholars consistently conclude that the humidity accelerates the degradation of performance.

Nardone et al.<sup>[11]</sup> conducted tests on the tensile strength of single-layer CFRP samples at 20 °C and 70 °C with 65% relative humidity, as well as the tensile properties of CFRP after being exposed to 30, 80, and 210 freeze-thaw cycles. The results indicate a significant decrease in tensile strength and ultimate strain as the temperature increases. The in-

fluence of a low number of freeze-thaw cycles on the mechanical properties of CFRP appears negligible, with only a slight reduction in tensile strength and ultimate strain observed after 210 cycles. Li et al.<sup>[12]</sup> conducted experiments that revealed a particular trend in the tensile strength of unidirectional CFRP plates after freeze-thaw cycles within the range of [−30—30 °C]: After 90 cycles, there was an initial decrease in the tensile strength, followed by an increase, and then another decrease, resulting in a 16% reduction in the tensile strength and an 18% decrease in the elastic modulus. These studies collectively highlight the significant detrimental effect of the combined influence of high and low temperature cycling along with humidity on the tensile properties of CFRP.

In addition to the influence of high and low temperature cycles and humidity, loading also plays a crucial role in affecting the properties of resin-based composites. Kafodya et al.<sup>[13]</sup> conducted research revealing that continuous bending loads had a noticeable impact on the tensile strength of CFRP composite panels when immersed in water and seawater. After two weeks of immersion, a significant decrease in the tensile strength was observed, followed by a gradual increase from four weeks to 12 weeks, and another substantial decline after 20 weeks of immersion. Xian et al.<sup>[14]</sup> further demonstrated that continuous bending loads led to the formation of micro-cracks at the resin-fiber interface of CFRP composites, resulting in reduced tensile strength. With an increase in the number of loading cycles, higher load levels accelerated the initiation and propagation of matrix and interface cracks, consequently hastening the decline in material strength. The above studies show that the coupling effect of high and low temperature cycle-humidity-load has significant influence on the tensile properties of EP-CFRP.

Currently, there is a limited number of reports addressing the combined impact of high and low temperature cycles, humidity, and loading. Most research predominantly focus on assessing the effects of high and low temperature cycling and humidity on the aging of composite materials, while often over-

looking the coupling effect of mechanical loading. In practical engineering structures, components typically endure the simultaneous influence of environmental conditions and mechanical loads, and these factors often exhibit certain degrees of interaction and mutual influence. Therefore, it is evidently insufficient to solely consider the effect of environmental factors or mechanical loads in isolation.

This paper focuses on the epoxy resin-based T700 carbon fiber reinforced composite material (EP-T700CFRP). Tensile strength tests and water absorption tests are conducted to investigate the changes in tensile properties and interface damage mechanisms. The study involves a comparison of experimental results obtained from different cycles of high and low temperature cycling under both no-load and various degrees of load conditions, in both soaking and anhydrous environments. This analysis aims to understand the variations in tensile properties and interface damage mechanisms of EP-T700CFRP plates under the combined influence of two factors: “High and low temperature cycle-humidity” and the three-factor coupling effect of “high and low temperature cycle-humidity-load”. Ultimately, a residual strength prediction model is developed through data fitting methods.

## 1 Test Materials and Methods

The EP-T700CFRP material investigated in this study was composed of T700-12K carbon fiber strands manufactured by Toray Corporation of Japan, serving as the reinforcement component, and epoxy resin FRD-YG-04 manufactured by Kunshan Yuba Composite Material Co., LTD, used as the matrix. The material was processed and cured through prepreg manual lamination and molding processes. The fundamental mechanical properties of the raw materials are detailed in Table 1 and Table 2. In accordance with the GB/T3354—2014 standard<sup>[15]</sup>, the specimens were prepared with dimensions of 230 mm×12.5 mm×2 mm. These specimens were cut along the fiber layering direction. To ensure the uniformity and reliability of the specimens, a selection process was conducted, removing

the specimens with surface defects while retaining those displaying a smooth and even filament distribution.

**Table 1 Performance index of T700SC-12K carbon fiber yarn**

Product name	Tensile strength/ MPa	Tensile modulus/ GPa	Elongation at break/%	Density / (g·cm <sup>3</sup> )
T700SC-12K	4 900	230	2.1	1.8

**Table 2 Performance index of FRD-YG-04 epoxy resin prepreg**

Product name	Glass transition temperature/°C	Tensile strength/MPa
FRD-YG-04	120—130	78

The paper investigates the impact of the coupling of high and low temperature cycling, humidity, and load on the tensile properties of EP-T700CFRP plates. The temperature conditions for the high and low temperature cycling experiments are determined based on typical domestic climate conditions, including a summer high temperature of 40 °C, an autumn normal temperature of 25 °C, and the lowest winter temperature of −40 °C. As structural composite materials typically bear loads up to 80% of their design allowable load, given the reduction in performance caused by moisture absorption during loading, it is advisable not to exceed 60% of the design allowable load for composite materials. In summary, this study examines two temperature cycle intervals: [−40—40 °C] and [−40—25 °C], under two environmental conditions, including soaking and anhydrous conditions, and three load conditions, comprising no load and loading levels at 30% and 60% of the ultimate load, respectively. The investigation focuses on the changes in the tensile properties of EP-T700CFRP plates under the combined effects of “high and low temperature cycle-humidity” and “high and low temperature cycle-humidity-load”. In addition to standard room temperature conditions, each test condition also involves 5, 10, 100, 200, and 300 cycles of high and low temperature fluctuations. Consequently, the “high and low

temperature cycle-humidity” two-factor coupled test comprises 4+1 operating conditions and 20+1 experimental groups, while the “high and low temperature cycle-humidity-loading” three-factor coupling test includes 8+1 operating conditions and 40+1 experimental groups, with 7 specimens prepared for each test group.

The experiment utilized the T-HWS-80U adjustable high and low temperature test chamber, manufactured by Dongguan Tianya Instrument Co., Ltd. The temperature control intervals for two high and low temperature cycle experiments were  $[-40-40\text{ }^{\circ}\text{C}]$  and  $[-40-25\text{ }^{\circ}\text{C}]$ . For each high and low temperature cycling experiment condition, a parallel comparison experiment involving two distinct humidity environments, soaking and anhydrous, was simultaneously conducted.

To realize the three-factor coupling effect of “high and low temperature cycle-humidity-loading”, a bending loading device, illustrated in Fig.1, was designed and manufactured based on the methodology described in Ref.[14].

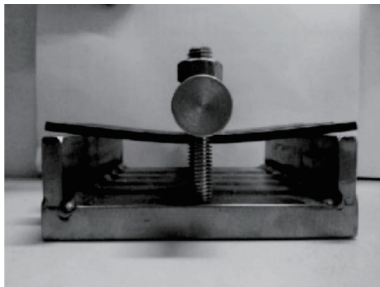


Fig.1 Bend loading device

According to Eq.(1), the corresponding deflection values for the bearing load level of 30% and 60% of the ultimate load are 1.276 mm and 2.552 mm, respectively.

$$\sigma_f = \frac{6Ehy}{L^2} \quad (1)$$

where  $\sigma_f$  is the applied bending load;  $E$ ,  $h$ ,  $y$  and  $L$  are the modulus of elasticity, thickness, deflection, and span, respectively.

Following the completion of the environmental experiments, the specimens underwent sequential water absorption rate and tensile strength testing. The water absorption test adhered to the standards

GB/T1462—2005<sup>[16]</sup> and HB7401—1996<sup>[17]</sup>. Initially, the specimens were placed in an oven at 70 °C and dried until reaching the engineering dry state. During the drying period, the specimens were weighed daily, and the dehumidification process was considered complete when the daily mass loss stabilized and did not exceed 0.02%. This indicated that the specimens had reached the engineering dry state. Subsequently, the specimens were exposed to room temperature conditions of 25 °C for hygroscopic treatment. The specimens were weighed daily for the first four days, and then the weighing frequency was shifted to once every three days. Daily weighing resumed when the rate of hygroscopic increment approached 0.05% of the daily mass increment. When the hygroscopic rate increment determined by three consecutive weightings falls below 0.05% of the daily mass increment, the specimen is considered to have reached a balanced hygroscopic state<sup>[17]</sup>. The water absorption of EP-CFRP can then be calculated using

$$w_i = \frac{G_i - G_0}{G_0} \times 100\% \quad (2)$$

where  $w_i$  is the equilibrium water absorption rate;  $G_0$  the quality in the dry engineering state; and  $G_i$  the quality of EP-CFRP after a certain time of hygroscopic treatment. When calculating the final water absorption rate of the specimen,  $G_i$  takes the mass at the equilibrium hygroscopic state.

The tensile strength test was conducted in accordance with the GB/T3354—2014 standard<sup>[15]</sup>. An ETM105D electric-hydraulic servo universal testing machine produced by Shenzhen Wance Test Equipment Co., Ltd. was used, with a loading rate of 2 mm/min.

## 2 Test Results and Analysis

### 2.1 High and low temperature cycle-humidity coupling effect

After the coupling effect of high and low temperature cycle-humidity, the tensile failure fracture of the specimen presents a relatively flat form, belonging to brittle failure<sup>[18]</sup>. The failure morphology is shown in Fig.2.

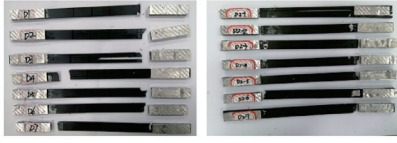


Fig.2 Damage morphology of specimens under high and low temperature cycle-humidity coupling effect

This paper presents the variation trends of tensile strength, equilibrium hygroscopicity, and tensile modulus for EP-T700CFRP one-way plates under the coupling effect of high and low temperature cycling and humidity, as depicted in Fig.3 and Fig.4. The tensile strength exhibits a pattern of initially decreasing, followed by an increase, and then another decrease. Meanwhile, equilibrium hygroscopicity displays an initial increase, followed by a decrease, and then another increase. Under the combined influence of high and low temperature cycling and humidity, the tensile strength of the specimens is noticeably lower compared with the anhydrous environment. Conversely, equilibrium hygroscopicity is significantly higher. The maximum decrease in tensile strength observed was 13.15%, while the maximum increase in equilibrium moisture absorption was 0.43%. The tensile modulus, however, underwent relatively minor changes.

In the initial stages of the coupling effect of high low temperature cycling and humidity (approximately five cycles), due to the significant difference in thermal expansion coefficients between the carbon fibers and the matrix, when there is a sudden

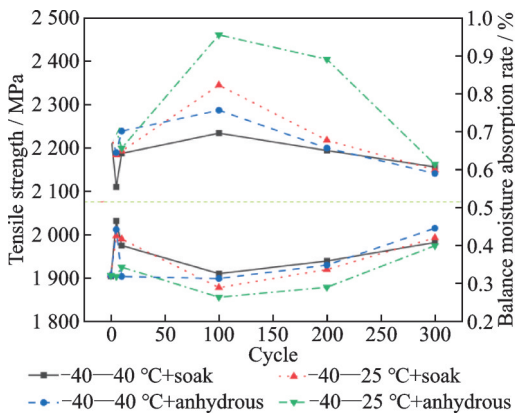


Fig.3 Relationship between tensile strength, moisture absorption and cycle period under high and low temperature cycle-humidity coupling effect

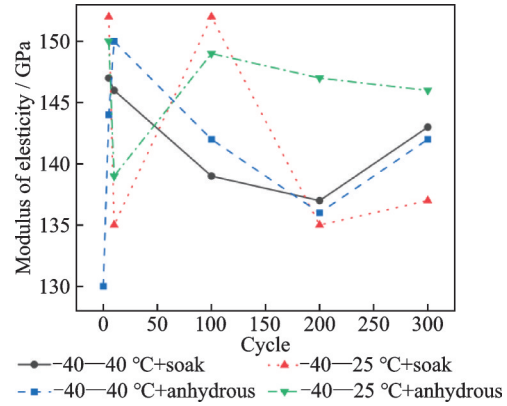


Fig.4 Relationship between elastic modulus and cycle period under high and low temperature cycle-humidity coupling effect

environmental change, significant thermal stresses and strains develop within the composite. This results in severe instantaneous cracking of the matrix<sup>[19]</sup>. During this period, the composite material's moisture absorption capability is enhanced, leading to an increase in equilibrium moisture content, and there is a noticeable decrease in tensile strength. After approximately ten cycles, the material undergoes subsequent curing effects at both room temperature and high temperature, resulting in an enhancement of interfacial bond strength<sup>[2]</sup>. This leads to a reduction in equilibrium moisture content, and the tensile strength returns to its initial state while exhibiting a growing trend. However, after cycling for more than 100 cycles, the continuous accumulation of the thermal stress and strain leads to further expansion of microcracks, an increase in equilibrium moisture content, and a subsequent decrease in tensile strength<sup>[20]</sup>.

### 2.2 High and low temperature cycle-humidity-load coupling effect

Under the coupling effect of high and low temperature cycle-humidity-load, the tensile failure of the specimen exhibits a form of loose wire splitting, which is characteristic of ductile failure<sup>[18]</sup>. The failure morphology is depicted in Fig.5.

(1) [ -40—40 °C ] high and low temperature cycle-humidity-load coupling effect

Fig.6 illustrates that under the coupling effect of high and low temperature cycling, humidity, and



Fig.5 Damage morphology of specimens under high and low temperature cycle-humidity load coupling effect

loading in the range of  $[-40-40\text{ }^{\circ}\text{C}]$ , the variation trend of tensile strength in the specimens aligns with the double-factor results. The overall trend for the specimens is a decrease initially, followed by an increase, and then another decrease. Concurrently, equilibrium hygroscopicity initially increases, then decreases, and then increases. It is worth noting that lower tensile strength corresponds to higher equilibrium hygroscopicity, indicating greater water absorption capacity within the material's capillaries, which also implies the presence of more microcracks in the material.

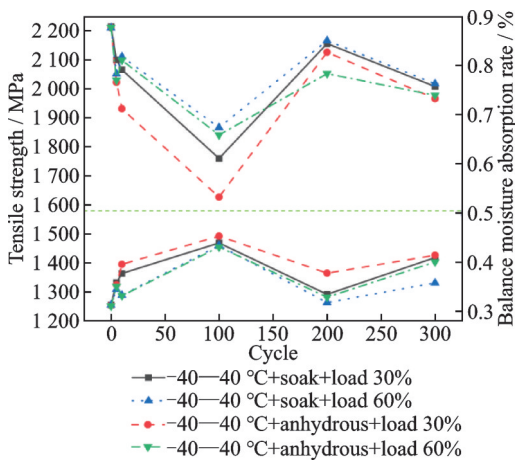


Fig.6 Relationship between tensile strength, moisture absorption and cycle period under  $[-40-40\text{ }^{\circ}\text{C}]$  temperature cycle-humidity-load coupling effect

Under the same load-holding conditions, after the same number of high and low temperature cycles, the tensile strength of specimens in a soaking environment is notably higher than that in an anhydrous environment, while equilibrium hygroscopicity is significantly lower than that in an anhydrous environment.

It can also be seen from Fig.6 that at the initial stage (about five cycles) of the coupling effect of the three factors of  $[-40-40\text{ }^{\circ}\text{C}]$  high and low

temperature cycle-humidity-load, when the environment is abrupt, the matrix will still have serious instantaneous cracking due to the thermal expansion coefficient which is quite different from the carbon fiber and the matrix, and the tensile strength will decline significantly. Compared with the coupling of two factors, when a load is introduced, the initial decline occurs over a longer cycle in the first round. During the initial stages, the cumulative effects of the thermal stress and thermal strain caused by environmental changes become more pronounced. The specimen's tensile strength significantly decreases after five cycles and continues to decline. After approximately 100 cycles, there is an inflection point where the tensile strength starts to increase (due to the post-curing effect of the composite material). It continues to rise until around the 200th cycle, after which there is a slight decrease in tensile strength. During this phase, internal microcracks and micropores in the specimen further expand, and there is a slight increase in equilibrium moisture content. Fig.7 demonstrates that the tensile modulus remains relatively stable.

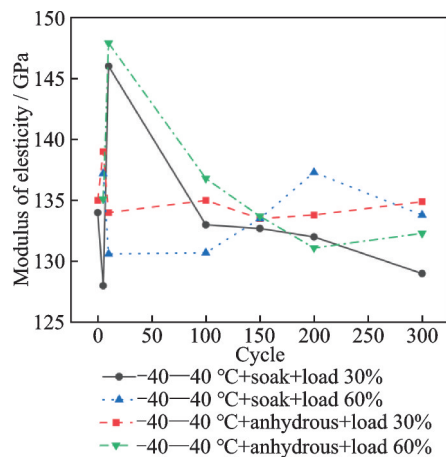


Fig.7 Relationship between elastic modulus and cycle period under  $[-40-40\text{ }^{\circ}\text{C}]$  temperature cycle-humidity-load coupling effect

(2)  $[-40-25\text{ }^{\circ}\text{C}]$  high and low temperature cycle-humidity-load coupling effect

According to Fig.8, the tensile strength of the specimens exhibits a different trend compared with the range of  $[-40-40\text{ }^{\circ}\text{C}]$ . Before 200 cycles, the

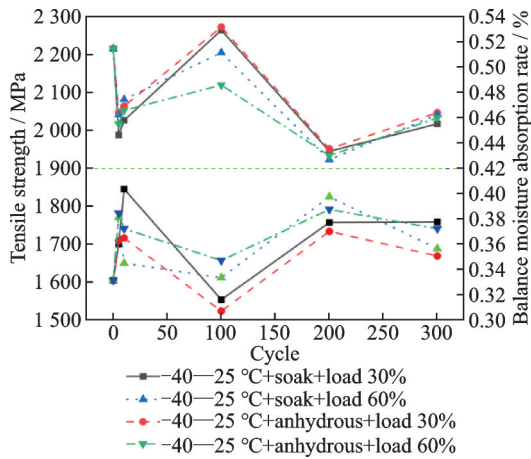


Fig.8 Relationship between tensile strength, moisture absorption and cycle period under  $[-40-25\text{ }^{\circ}\text{C}]$  temperature cycle-humidity-load coupling effect

trend in tensile strength changes is consistent with the combined effect of high and low temperature cycle-humidity on tensile strength. From 200 cycles to 300 cycles, a second slight increase in tensile strength is observed. Overall, it exhibits a changing trend in four stages: Initially decreasing, then increasing, followed by another decrease, and finally, a second increase. The equilibrium moisture absorption rate also follows a corresponding pattern of initially rising, then falling, followed by another increase, and then another decrease. For the same soaking environment or anhydrous environment, after the same cycle of high and low temperature, the tensile strength of 60% load is less than the tensile strength of 30% load, and the equilibrium moisture absorption rate is correspondingly larger. Fig.9 shows that the tensile modulus does not change much.

Based on the above experimental results, there exists a certain correlation between external load and moisture absorption in composite materials: After subjecting laminated plates to the same humid thermal cycle, the higher the load level, the greater the moisture absorption rate of composite materials, and the more pronounced the decline in tensile strength. This phenomenon can be attributed to the presence of initial cracks, pores, and other defects within the resin matrix composites. The application of load induces stress concentration at these defects,

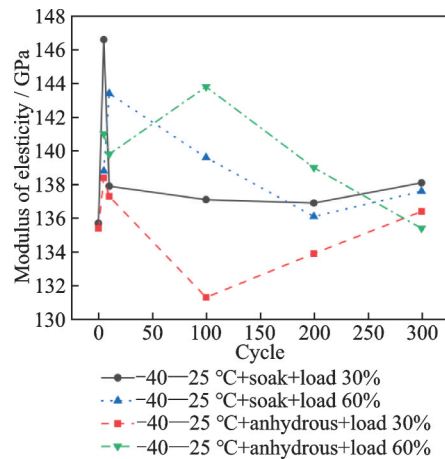


Fig.9 Relationship between elastic modulus and cycle period under  $[-40-25\text{ }^{\circ}\text{C}]$  temperature cycle-humidity-load coupling effect

accelerating crack formation and expansion while promoting further moisture absorption within the matrix. This mechanism can be termed “stress cracking”.

As moisture absorption increases, the mismatch between moisture and thermal expansion between the fibers and the resin matrix becomes more severe, leading to shear internal stress at the interface. When this shear stress surpasses the bonding force holding the interface together, interface debonding and delamination occur, further enhancing moisture absorption. This mechanism can be termed “stress-induced debonding”<sup>[21]</sup>.

Consequently, due to external load, moisture absorption is promoted in these two aspects, resulting in an increased rate of hygroscopicity and equilibrium hygroscopicity within the material. The higher the applied load, the more pronounced the promoting effect on the material’s hygroscopicity. In summary, the hygroscopic process of composites under external loading constitutes a self-accelerating vicious cycle, and the combined influence of external loading force and hygroscopic force accelerates the damage to the strength of composites.

### 3 Analysis of Strength Damage Model

The variation in tensile strength is primarily in-

fluenced by factors such as the high and low temperature intervals<sup>[22]</sup>, the high and low temperature cycling<sup>[23]</sup>, environmental humidity, and external load<sup>[24]</sup>. This variation comprehensively reflects the damage to the matrix and the interfacial bonding properties of composites. In this study, two temperature cycle intervals of [−40—40 °C] and [−40—25 °C], as well as two environmental conditions involving soaking and anhydrous, were considered to investigate the pattern of change in EP-T700CFRP composite plates subjected to different cycles of high and low temperature and various external load levels. The residual tensile strength model can be expressed as

$$R(n) = f(n, s) \tag{3}$$

where  $R(n)$  is the residual tensile strength of EP-CFRP after high and low temperature cycles;  $n$  the number of high and low temperature cycles, and  $s$  the stress ratio of applied load.

According to the design requirements of composite structures for domestic aircraft, the general design strength is 130% of the design load. After conversion, when the strength of composite laminates decreases by 23%, it can be considered as strength failure. Assuming that  $\sigma_0$  is the initial tensile strength of EP-CFRP laminates at room temperature, the ultimate tensile strength is  $\sigma_f = (1 - 0.23)\sigma_0 = 0.77\sigma_0$ . Therefore, the boundary conditions satisfying Eq.(3) are

$$R(0) = \sigma_0 \tag{4}$$

$$R(n_f) = \sigma_f = 0.77\sigma_0 \tag{5}$$

Based on the cumulative damage theory<sup>[25]</sup>, the damage amount of a high and low temperature cycles test can be defined as

$$\Delta D_i = A \cdot [R(i - 1) - R(i)] \tag{6}$$

where  $\Delta D_i$  is the injury caused by cycle  $i$ ;  $R(i)$  the residual tensile strength of EP-CFRP after  $i$  cycles, and  $A$  the material coefficient.

The cumulative damage after  $n$  cycles is

$$D_n = \sum_{i=1}^n \Delta D_i \tag{7}$$

where  $D_n$  is the accumulated damage after  $n$  cycles.

When the number of cycles is  $n = n_f$ , the speci-

men has reached the critical damage state, and the cumulative value of damage failure is

$$D_{cr} = \sum_{i=1}^n A \cdot [R(i - 1) - R(i)] = A \cdot [R(0) - R(n_f)] \tag{8}$$

Substituted into the boundary conditions (4) and (5), the critical cumulative damage value  $D_{cr}$  is

$$D_{cr} = A \cdot (\sigma_0 - \sigma_f) \tag{9}$$

Assuming that the critical damage limit value of the damage failure of EP-CFRP specimens after cyclic test is 1, Eq.(9) can be written as follows

$$A = \frac{1}{\sigma_0 - \sigma_f} \tag{10}$$

Since the residual tensile strength of the composite component failure is  $\sigma_f = 0.77\sigma_0$ , combined with Eqs.(6, 7, 10), the cumulative damage model of the residual tensile strength after the cycle test is

$$R(n) = \sigma_0 - (\sigma_0 - \sigma_f) \cdot D_n = \sigma_0 - 0.23\sigma_0 \cdot D_n \tag{11}$$

The determination of the damage function is a key aspect of establishing the damage model. Based on the tensile test results, the cumulative damage strength of EP-T700CFRP under four different conditions: [−40—40 °C] soak, [−40—40 °C] anhydrous, [−40—25 °C] soak, and [−40—25 °C] anhydrous, was analyzed. The damage function  $D_n$  is described based on two factors: The cycles ( $n$ ) and the load levels ( $s$ ).

$$D_n = f(n) \cdot g(s) \tag{12}$$

where  $f(n)$  represents the influence of cycle number ( $n$ ) on cumulative damage strength, and  $g(s)$  the influence of different load levels ( $s$ ) on cumulative damage strength. Therefore, the boundary conditions are defined as  $f(0) = 0$  and  $g(0) = 1$ .

First, consider the impact of the number of cycles ( $n$ ) on the damage function  $D_n$ . As ten cycles of high and low temperature cycles are taken as a dividing point, there is a significant difference in the cumulative damage variation of T700CFRP tensile strength before and after this point. Therefore, an approach involving piecewise functions is employed. A quadratic polynomial is used to describe  $D_n$  before ten cycles, and a cubic polynomial is used after ten cycles. It is important to note that there is a bound-



ary condition  $g(0)=1$ , which means that the damage function curve under no load is the same as the  $f(n)$  curve.

Next, the influence of the load levels ( $s$ ) on the damage function  $D_n$  is considered. The average cumulative damage under three different load levels is calculated and the multiplicative relationship among them is determined.  $g(0)=1$  is used as a reference point, values for  $g(30\%)$  and  $g(60\%)$  are obtained, and  $g(s)$  is described using quadratic polynomials.

For example, given  $[-40-40\text{ }^\circ\text{C}]$  soak, the form of the damage function  $D_n$  curve is as follows

$$D_n = f(n) \cdot g(s) = \begin{cases} (an^2 + bn)(As^2 + Bs + C) & n \leq 10 \\ (cn^3 + dn^2 + kn + l)(As^2 + Bs + C) & n > 10 \end{cases} \quad (13)$$

where  $f(n) = \begin{cases} an^2 + bn & n \leq 10 \\ cn^3 + dn^2 + kn + l & n > 10 \end{cases}$ ,  $g(s) = As^2 + Bs + C$ ;  $a, b, c, d, k, l, A, B, C$  represent the polynomial coefficients.

Table 3 contains the cumulative damage strength under  $[-40-40\text{ }^\circ\text{C}]$  soaking condition. By calculating the average damage strength values for each load level and considering the boundary condition  $g(0)=1$ ,  $g(30\%)=2.5342$  and  $g(60\%)=2.2616$  are obtained. Therefore, the expression for  $g(s)$  is given as follows

$$g(s) = -10.0384s^2 + 8.1256s + 1 \quad (14)$$

**Table 3 Cumulative damage strength at  $[-40-40\text{ }^\circ\text{C}]$  soak**

$n$	No load	Load 30%	Load 60%
0	0	0	0
5	0.372 200	0.219 20	0.315 7
10	0.082 400	0.287 64	0.207 6
100	-0.009 486	0.887 20	0.683 6
200	0.160 500	0.112 60	0.100 6
300	0.144 700	0.394 70	0.389 3
Average	0.125 000	0.316 90	0.282 8
Calibrate	1	2.534 20	2.261 6

Fig.10 shows the damage function curves under three different load levels, while Table 4 provides the polynomial coefficients for this damage function. After averaging the coefficients to obtain the damage curve under average loading, the damage function curve under no load is calibrated using  $g(s)$ . Finally, this calibration allows for the prediction of damage function curves under three different loading conditions, as shown in Fig.11(a).

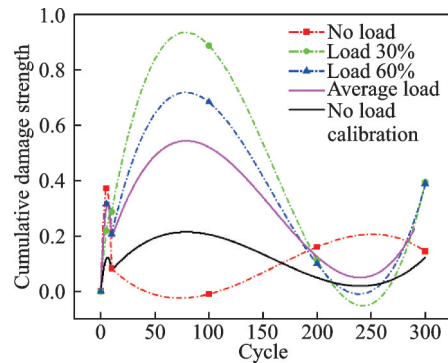


Fig.10 No load curve calibration at  $[-40-40\text{ }^\circ\text{C}]$  soak

**Table 4 Polynomial coefficients at  $[-40-40\text{ }^\circ\text{C}]$  soak**

$s$	$a$	$b$	$c$	$d$	$k$	$l$
0	-0.013 240	0.140 60	-8.142E-08	3.96E-05	-0.004 469	0.123 20
30%	-0.003 017	0.058 93	4.437E-07	-0.000 213 4	0.025 210	0.056 42
60%	-0.008 477	0.105 50	3.521E-07	-0.000 167 7	0.019 820	0.025 78
Average load	-0.008 245	0.101 70	2.381E-07	-0.000 113 8	0.013 520	0.068 47
No load calibration	-0.003 253	0.040 12	9.396E-08	-4.492E-05	0.005 335	0.027 02

The same method is applied to other operating conditions to obtain corresponding cumulative damage strength prediction models, as shown in Fig.11. The polynomial coefficients for the corresponding cumulative damage function are given in Table 5.

Taking both aspects into account, all coefficients in the damage function expression were determined. Substituting Eq.(13) into Eq.(11), the predictive model for the cyclic residual tensile strength of EP-CFRP composite materials under different operating conditions was obtained as

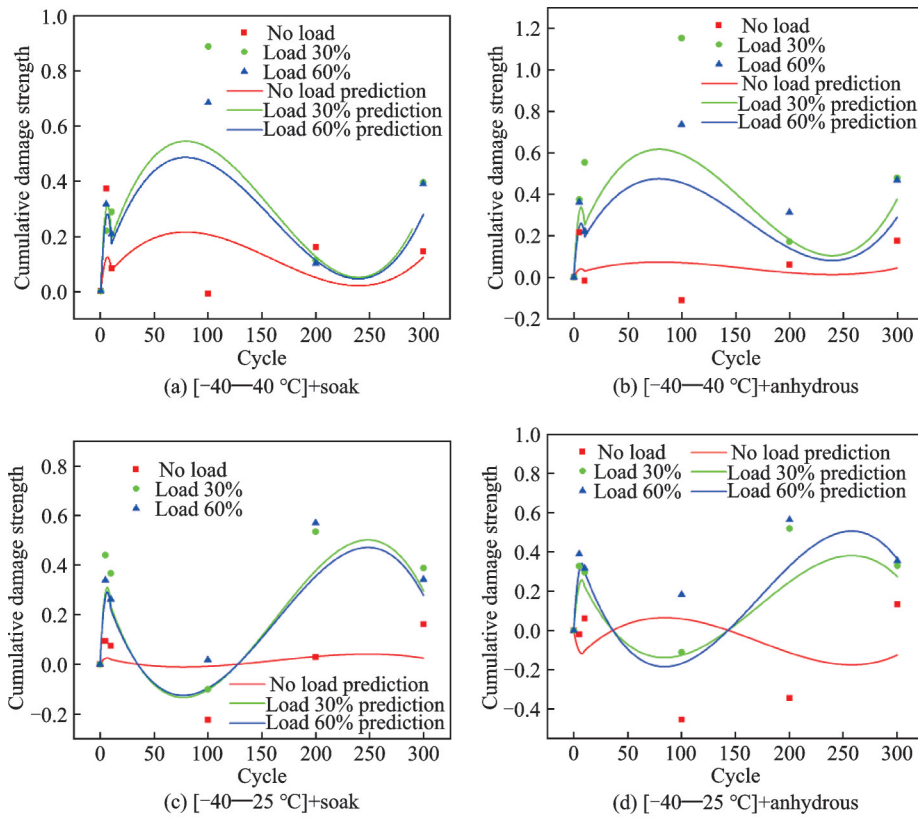


Fig.11 Predicted cumulative damage strength curves under different conditions

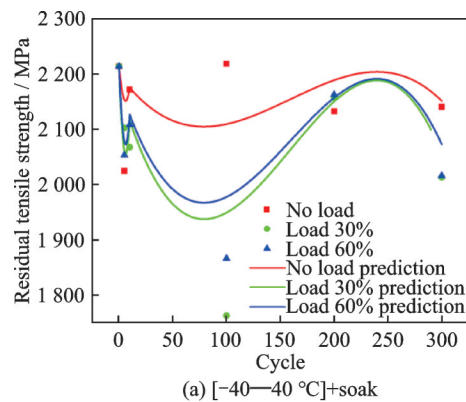
Table 5 Polynomial coefficients

Working condition	<i>a</i>	<i>b</i>	<i>c</i>	<i>d</i>	<i>k</i>	<i>l</i>	<i>A</i>	<i>B</i>
[-40-40 °C]+soak	-0.003 253	0.040 12	9.396E-08	-4.492E-05	0.005 335	0.027 02	-10.038 4	8.125 6
[-40-40 °C]+anhydrous	-0.007 637	0.101 6	2.47E-07	-1.180E-04	0.014 02	0.123 7	-52.479 0	40.692 7
[-40-25 °C]+soak	-0.006 962	0.093 04	-2.520E-07	1.231E-04	-0.014 49	0.367 0	-66.552 0	57.437 4
[-40-25 °C]+anhydrous	-0.004 774	0.070 20	-1.986E-07	0.000 101 8	-0.012 91	0.343 5	13.653 2	-14.655 2

$$R(n) = \begin{cases} \sigma_0 - 0.23\sigma_0 \cdot (an^2 + bn) \cdot (ks^2 + ls + 1) & n \leq 10 \\ \sigma_0 - 0.23\sigma_0 \cdot (cn^3 + dn^2 + cn + d) \cdot (ks^2 + ls + 1) & n > 10 \end{cases} \quad (15)$$

In Eq.(15), the polynomial coefficients under different operating conditions are referenced from Table 5. The comparison between the residual tensile strength values calculated based on the respective predictive models in Eq.(15) and experimental results is illustrated in Fig.12. The residual tensile strength values calculated by this predictive model closely align with the experimental results, confirming its effectiveness. Therefore, the damage model proposed in this study can be used to predict the tensile strength of epoxy resin-based carbon fiber-reinforced composites after the coupling effect of high

and low temperature cycle-humidity-load coupling effect.



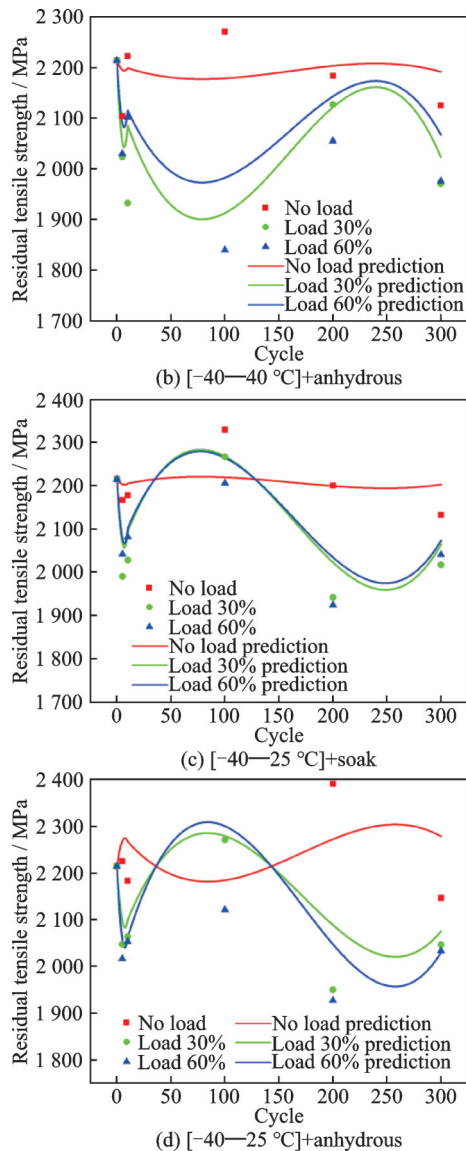


Fig.12 Residual strength prediction models under different conditions

## 4 Conclusions

The variation law of tensile strength, interface damage mechanism and residual strength damage model of EP-T700CFRP sheet under the coupling action of high and low temperature-humidity-applied tensile load are studied according to the experiment results. It leads to the following conclusion:

(1) Under the coupling two factors of “high and low temperature cycle-humidity” and the three factors of “high and low temperature cycle-humidity-load”, the tensile strength of EP-CFRP decreases first and then increases and then decreases with the

increase of the temperature cycles. However, when the peak and valley values of the tensile strength appear, their corresponding cycles differ greatly. In all the processes, humidity and load level have little influence on the tensile modulus of EP-CFRP.

(2) By comparing the tensile strength and equilibrium hygroscopicity of the materials, it can be seen that the micro-cracks at the interface between the resin matrix and the fiber are the main reason for the later strength reduction of the materials. The coupling effect of humidity and load promotes the propagation of cracks and obviously weakens the tensile properties of the resin-based carbon fiber composites.

(3) Based on the cumulative damage theory and the nonlinear fitting method, the damage functions of EP-T700CFRP composite plates are calibrated for conditions with two temperature cycles of  $[-40-40\text{ °C}]/[-40-25\text{ °C}]$  and two environmental humidities of soaking and anhydrous, leading to a reasonable residual strength prediction model.

## References

- [1] ATTAHU C Y, AN L L, LI Z Q, et al. Influence of shim layers on progressive failure of a composite component in composite-aluminum bolted joint in aerospace structural assembly[J]. Transactions of Nanjing University of Aeronautics & Astronautics, 2018, 35 (1): 188-202.
- [2] GAO Y, DONG S L, WANG H S, et al. Effect of vacuum thermal cycling on mechanical and physical properties of an epoxy matrix composite[J]. Advanced Materials Research, 2011, 415/416/417: 2236-2239.
- [3] YU Q, CHEN P, GAO Y, et al. Effects of vacuum thermal cycling on mechanical and physical properties of high performance carbon/bismaleimide composite[J]. Materials Chemistry and Physics, 2011, 130 (3): 1046-1053.
- [4] MENG J X, WANG Y, YANG H Y, et al. Mechanical properties and internal microdefects evolution of carbon fiber reinforced polymer composites: Cryogenic temperature and thermocycling effects[J]. Composites Science and Technology, 2020, 191: 108083.

- [5] LORD H W, DUTTA P K. On the design of polymeric composite structures for cold regions applications[J]. *Journal of Reinforced Plastics and Composites*, 1988, 7(5): 435-458.
- [6] LI B, CHEN J Z, LV Y, et al. Influence of humidity on fatigue performance of CFRP: A molecular simulation[J]. *Polymers*, 2021, 13(1): 140.
- [7] GÁLVEZ P, DE ARMENTIA S L, ABENOJAR J, et al. Effect of moisture and temperature on thermal and mechanical properties of structural polyurethane adhesive joints[J]. *Composite Structures*, 2020, 247(11): 112443.
- [8] CHEN Z B, HUANG P Y, YAO G W, et al. Experimental study on fatigue performance of RC beams strengthened with CFRP under variable amplitude overload and hot-wet environment[J]. *Composite Structures*, 2020, 244: 112308.
- [9] DE PARSCAU DU PLESSIX B, JACQUEMIN F, LEFÉBURE P, et al. Characterization and modeling of the polymerization-dependent moisture absorption behavior of an epoxy-carbon fiber-reinforced composite material[J]. *Journal of Composite Materials*, 2016, 50(18): 2495-2505.
- [10] YALAGACH M, FUCHS P F, ANTRETTETTER T, et al. Thermal and moisture dependent material characterization and modeling of glass fiber reinforced epoxy laminates[J]. *Sensors & Transducers Journal*, 2021, 248(1): 1-9.
- [11] NARDONE F, LUDOVICO M D I, BASALO F J D C Y, et al. Tensile behavior of epoxy based FRP composites under extreme service conditions[J]. *Composites Part B: Engineering*, 2012, 43(3): 1468-1474.
- [12] LI H, XIAN G J, LIN Q, et al. Freeze-thaw resistance of unidirectional-fiber-reinforced epoxy composites[J]. *Journal of Applied Polymer Science*, 2012, 123(6): 3781-3788.
- [13] KAFODYA I, XIAN G, LI H. Durability study of pultruded CFRP plates immersed in water and seawater under sustained bending: Water uptake and effects on the mechanical properties[J]. *Composites Part B: Engineering*, 2015, 70: 138-148.
- [14] XIAN G J, GUO R, LI C G. Combined effects of sustained bending loading, water immersion and fiber hybrid mode on the mechanical properties of carbon/glass fiber reinforced polymer composite[J]. *Composite Structures*, 2022, 281: 115060.
- [15] Standardization Administration of the People's Republic of China. Test method for tensile properties of oriented fiber reinforced polymer matrix composites: GB/T3354—2014[S]. Beijing: [s.n.], 2014.
- [16] Standardization Administration of the People's Republic of China. Test method for the water absorption of fiber reinforced plastic: GB/T1462 — 2005[S]. Beijing: [s.n.], 2005.
- [17] People's Republic of China Aviation Industry Standard. Test method for moisture absorption of resin matrix composite laminates in hot and humid environment: HB7401—1996[S]. Beijing: [s.n.], 1996.
- [18] ZHANG M Y, LI K Z, SHI X H, et al. Effect of vacuum thermal cyclic exposures on the carbon/carbon composites[J]. *Vacuum*, 2015, 122: 236-242.
- [19] KHALILI S M R, NAJAFI M, ESLAMI-FARSANI R. Effect of thermal cycling on the tensile behavior of polymer composites reinforced by basalt and carbon fibers[J]. *Mechanics of Composite Materials*, 2017, 52(6): 807-816.
- [20] WANG S Q, DONG S L, GAO Y, et al. Thermal ageing effects on mechanical properties and barely visible impact damage behavior of a carbon fiber reinforced bismaleimide composite[J]. *Materials & Design*, 2017, 115: 213-223.
- [21] WAN Y Z, WANG Y L, LUO H L, et al. Moisture absorption behavior of C3D/EP composite and effect of external stress[J]. *Materials Science and Engineering: A*, 2002, 326(2): 324-329.
- [22] ZHANG C, BINIENDA W K, MORSCHER G N, et al. Experimental and FEM study of thermal cycling induced microcracking in carbon/epoxy triaxial braided composites[J]. *Composites Part A: Applied Science and Manufacturing*, 2013, 46: 34-44.
- [23] ZHANG A, LI D H, LU H B, et al. Qualitative separation of the effect of voids on the bending fatigue performance of hygrothermal conditioned carbon/epoxy composites[J]. *Materials & Design*, 2011, 32(10): 4803-4809.
- [24] HONG B, XIAN G J, LI H. Comparative study of the durability behaviors of epoxy- and polyurethane-based CFRP plates subjected to the combined effects of sustained bending and water/seawater immersion[J]. *Polymers*, 2017, 9(11): 603.
- [25] SHIINO M Y, FARIA M C M, BOTELHO E C, et al. Oliveira, assessment of cumulative damage by using ultrasonic c-scan on carbon fiber/epoxy composites

under thermal cycling[J]. Materials Research, 2012, 15(4): 495-499.

**Acknowledgements** This work was financially supported by the Natural Science Foundation of Sichuan Province (No. 2022NSFSC0317) and Key Laboratory of Icing and Anti/De-icing of Aircraft Project (No.IADL20190404).

**Author** Dr. SHI Jianjun is a double doctorate jointly trained by China and France. He received his two Ph.D. degrees in engineering mechanics from Southwest Jiaotong University in Chengdu, China in 2014 and in mechanical engineering from French-Comte University in France. From 2014 to present, he has been with the Department of Engineering Mechanics, College of Civil Engineering and Architecture, Southwest University of Science and Technology,

where he is currently an associate professor. His research has focused on composite material (structural) mechanics, multi-physical field coupling simulation, etc.

**Author contributions** Dr. SHI Jianjun designed the study, investigated related literature, conducted the analysis, interpreted the results and wrote the manuscript. Mr. WANG Wenze contributed to data and analyses for the predictive model of the residual strength. Mr. WEI Wangcheng and Mr. LIU Yifan contributed to the discussion and background of this research. All authors commented on the manuscript draft and approved the submission.

**Competing interests** The authors declare no competing interests.

(Production Editor: XU Chengting)

## 树脂基纤维复合材料在湿热耦合及载荷-湿热耦合环境下的损伤分析

石建军, 王文泽, 魏王程, 刘一凡

(西南科技大学土木工程与建筑学院, 绵阳 621010, 中国)

**摘要:**研究了环氧树脂基碳纤维增强复合材料(EP-CFRP)在高低温-湿度-拉伸载荷耦合作用下的损伤情况。考虑了两个高低温循环间隔( $[-40\sim 40\text{ }^{\circ}\text{C}]/[-40\sim 25\text{ }^{\circ}\text{C}]$ )、两种湿度条件(浸泡在水中/无水)和3个荷载水平(无荷载/30%极限荷载/60%极限荷载)以及它们之间的耦合效应。结果表明,这3个因素对EP-CFRP的耐久性均有显著影响。这些因素的耦合效应对抗拉强度的影响较大,而对拉伸模量的影响较小。树脂基体与纤维界面产生的微裂纹被证明是后期强度降低的主要原因。湿度和拉伸载荷的耦合效应促进了裂纹的膨胀,加剧了对EP-CFRP的损伤。基于累积损伤理论,采用非线性拟合方法标定了EP-CFRP在3因素耦合作用下的剩余强度损伤模型。

**关键词:**碳纤维增强复合材料; 高低温循环; 湿度; 拉伸性能; 剩余强度模型